

From global fits of neutrino data to constrained sequential dominance

Fredrik Björkeröth* and Stephen F. King†

*School of Physics and Astronomy, University of Southampton,
Southampton, SO17 1BJ, United Kingdom*

Constrained sequential dominance (CSD) is a natural framework for implementing the see-saw mechanism of neutrino masses which allows the mixing angles and phases to be accurately predicted in terms of relatively few input parameters. We perform a global analysis on a class of CSD(n) models where, in the flavour basis, two right-handed neutrinos are dominantly responsible for the “atmospheric” and “solar” neutrino masses with Yukawa couplings to $(\nu_e, \nu_\mu, \nu_\tau)$ proportional to $(0, 1, 1)$ and $(1, n, n - 2)$, respectively, where n is a positive integer. With two right-handed neutrinos, we find excellent agreement with experiment ($\chi^2 \lesssim 1$) for CSD(3) and CSD(4) where the entire PMNS mixing matrix is controlled by a single phase η , which takes simple values, leading to accurate predictions for mixing angles and the magnitude of the oscillation phase $|\delta_{CP}|$. We carefully study the perturbing effect of a third “decoupled” right-handed neutrino, leading to a bound on the lightest physical neutrino mass $m_1 \lesssim 1$ meV for the viable cases, corresponding to a normal neutrino mass hierarchy. We also discuss a direct link between the oscillation phase δ_{CP} and leptogenesis in CSD(n) due to the same see-saw phase η appearing in both the neutrino mass matrix and leptogenesis.

*E-mail: F.Bjorkeroth@soton.ac.uk

†E-mail: king@soton.ac.uk

1. Introduction

The astonishingly accurate measurement of the third lepton mixing angle, the so-called reactor angle $\theta_{13} \approx 8.5^\circ \pm 0.2^\circ$ [1], signals the start of the precision era for neutrino physics. Over the coming years, all three lepton mixing angles are expected to be measured with increasing precision. A first tentative hint for a value of the CP-violating phase $\delta_{CP} \sim -\pi/2$ has also been reported in global fits [2–4]. However the mass squared ordering (normal or inverted), the scale (mass of the lightest neutrino) and nature (Dirac or Majorana) of neutrino mass so far all remain unknown.¹

On the theory side, there are many possibilities for the origin of light neutrino masses m_i and mixing angles θ_{ij} . Perhaps the simplest and most elegant idea is the classical see-saw mechanism, in which the observed smallness of neutrino masses is due to the heaviness of right-handed Majorana neutrinos [5],

$$m^\nu = m^D M_R^{-1} (m^D)^T, \quad (1.1)$$

where m^ν is the light effective left-handed² Majorana neutrino mass matrix (i.e. the physical neutrino mass matrix), m^D is the Dirac mass matrix (in LR convention) and M_R is the (heavy) Majorana mass matrix. Although the see-saw mechanism generally predicts Majorana neutrinos, it does not predict the “mass hierarchy”, nor does it yield any understanding of lepton mixing. In order to overcome these deficiencies, the see-saw mechanism must be supplemented by other ingredients.

One attractive idea, depicted in Fig. 1, is that the Standard Model (SM) is supplemented by three right-handed neutrinos which contribute sequentially to the light effective neutrino mass matrix. The idea of such a “sequential dominance” (SD) [6] is that one dominant right-handed neutrino ν_R^{atm} of mass M_{atm} is mainly responsible for the heaviest atmospheric neutrino mass m_3 , while a second subdominant right-handed neutrino ν_R^{sol} of mass M_{sol} mainly gives the solar neutrino mass m_2 . A third, approximately decoupled, right-handed neutrino ν_R^{dec} of mass M_{dec} is responsible for the lightest neutrino mass m_1 . In the diagonal basis, $M_R = \text{diag}(M_{\text{atm}}, M_{\text{sol}}, M_{\text{dec}})$ where the Dirac mass matrix is constructed from three columns $m^D = (m_{\text{atm}}^D, m_{\text{sol}}^D, m_{\text{dec}}^D)$, applying the see-saw formula in Eq. 1.1 gives,

$$m^\nu = \frac{m_{\text{atm}}^D (m_{\text{atm}}^D)^T}{M_{\text{atm}}} + \frac{m_{\text{sol}}^D (m_{\text{sol}}^D)^T}{M_{\text{sol}}} + \frac{m_{\text{dec}}^D (m_{\text{dec}}^D)^T}{M_{\text{dec}}}, \quad (1.2)$$

where

$$\frac{(m_{\text{atm}}^D)^\dagger m_{\text{atm}}^D}{M_{\text{atm}}} > \frac{(m_{\text{sol}}^D)^\dagger m_{\text{sol}}^D}{M_{\text{sol}}} \gg \frac{(m_{\text{dec}}^D)^\dagger m_{\text{dec}}^D}{M_{\text{dec}}}, \quad (1.3)$$

leading immediately to the prediction of a normal mass hierarchy of physical neutrino masses $m_3 > m_2 \gg m_1$.

¹The first two attributes are commonly referred to jointly as the “mass hierarchy”, although really they are separate questions.

²We have ignored the overall physically irrelevant phase of -1.

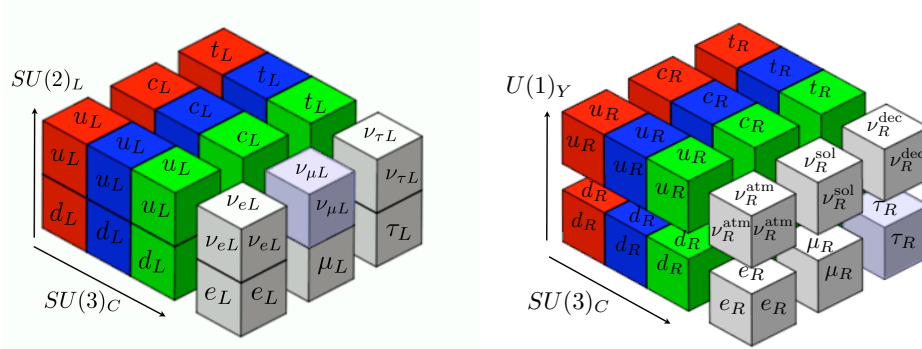


Fig. 1: The Standard Model (SM) with three right-handed neutrinos defined as $(\nu_R^{\text{atm}}, \nu_R^{\text{sol}}, \nu_R^{\text{dec}})$ which in sequential dominance are mainly responsible for the m_3, m_2, m_1 physical neutrino masses, respectively.

The observed pattern of lepton mixing angles can be understood in the above SD framework as follows. In the diagonal charged lepton and right-handed neutrino mass basis, if the dominant “atmospheric” right-handed neutrino ν_R^{atm} has couplings $(m_{\text{atm}}^D)^T = (0, a_1, a_2)$ to $(\nu_e, \nu_\mu, \nu_\tau)$, then this implies $\tan \theta_{23} \sim a_1/a_2$ [6] and a bound $\theta_{13} \lesssim m_2/m_3$ [7]. The subdominant “solar” right-handed neutrino ν_R^{sol} couplings $(m_{\text{sol}}^D)^T = (b_1, b_2, b_3)$ to $(\nu_e, \nu_\mu, \nu_\tau)$ further yield $\tan \theta_{12} \sim \sqrt{2}b_1/(b_2 - b_3)$ [6, 7]. The lepton mixing angles are of course insensitive to the “decoupled” right-handed neutrino couplings.

In order to obtain sharp predictions for lepton mixing angles, the relevant Yukawa coupling ratios need to be fixed, for example using vacuum alignment of family symmetry breaking flavons (for reviews see e.g. [8–11]). The first attempt to use vacuum alignment within an $SU(3)$ family symmetry to predict maximal atmospheric mixing ($\tan \theta_{23} \sim 1$) from equal dominant right-handed neutrino couplings $(m_{\text{atm}}^D)^T = (0, a, a)$ was discussed in [12]. Subsequently, constrained sequential dominance (CSD) [13] was proposed to explain tri-bimaximal (TB) mixing with a zero reactor angle by using vacuum alignment to fix the subdominant “solar” right-handed neutrino couplings to $(\nu_e, \nu_\mu, \nu_\tau)$ to also be equal up to a sign³, namely $(m_{\text{sol}}^D)^T = (b, b, -b)$.

Following the measurement of the reactor angle, other types of CSD have been proposed, with the dominant right-handed “atmospheric” couplings as above,

$$(m_{\text{atm}}^D)^T = (0, a, a) \quad (1.4)$$

and hence an approximate maximal atmospheric angle $\tan \theta_{23} \sim a_1/a_2 \sim 1$, while proposing alternative subdominant “solar” right-handed neutrino couplings as follows:

- CSD(2): $(m_{\text{sol}}^D)^T = (b, 2b, 0)$ [15].
- CSD(3): $(m_{\text{sol}}^D)^T = (b, 3b, b)$ [16].
- CSD(4): $(m_{\text{sol}}^D)^T = (b, 4b, 2b)$ [16, 17].

³Note that $(0, a, a) \cdot (b, b, -b) = 0$. This orthogonality is related to the fact that CSD(1) respects form dominance, since columns of the Dirac mass matrix in the flavour basis are proportional to the columns of the unitary PMNS mixing matrix [14].

All these examples maintain an approximate trimaximal value for the solar leptonic angle $\tan \theta_{12} \sim \sqrt{2}b_1/(b_2 - b_3) \sim 1/\sqrt{2}$, while switching on the reactor angle. Since experiment indicates that the bound $\theta_{13} \lesssim m_2/m_3$ is almost saturated, these schemes also require certain phase choices $\arg(b/a)$ in order to achieve the desired reactor angle, leading to predictions for the CP-violating phase δ_{CP} .⁴

From the point of view of discrete family symmetry models, the above approach is sometimes referred to as “indirect” since the required vacuum alignments completely break the family symmetry [19]. Such “indirect” models are highly predictive and do not require such large discrete groups as the “direct” models which use only vacuum alignments which preserve a subgroup $Z_2 \times Z_2$ in the neutrino sector (the so-called Klein symmetry) and Z_3 in the charged lepton sector, where such an approach requires $\Delta(6N^2)$ for large values of N [20–23].⁵

In this paper we perform a dedicated global analysis of the general class of CSD(n) models, independently of any detailed model, allowing the positive integer n to take any value. Thus we consider the “atmospheric” right-handed neutrino to have the usual couplings in Eq. 1.4, while the subdominant “solar” right-handed neutrino has couplings to $(\nu_e, \nu_\mu, \nu_\tau)$ given by the general formula:

$$\text{CSD}(n) : \quad (m_{\text{sol}}^D)^T = (b, nb, (n-2)b), \quad (1.5)$$

where n is any positive integer. This is a generalisation of the above examples studied in the literature so far for $n = 2, 3, 4$, including the original CSD identified here as CSD(1). After the see-saw mechanism has been implemented, with just two right-handed neutrinos, the light effective Majorana neutrino mass matrix depends on just two mass parameters m_a and m_b and a relative phase η . For each value of n we perform a global fit to the input parameters, which in the case of two right-handed neutrinos, consists of just two masses and one phase (three real input parameters) which are used to fit the observed data of two mass squared differences, and three lepton angles (five observed parameters).

The CP phase δ_{CP} emerges from the global fit as a genuine prediction. Moreover, with just two right-handed neutrinos in CSD(n), there is a direct link between the oscillation phase δ_{CP} and the leptogenesis phase since there is only one phase η in the see-saw matrices which is responsible for both. The more general case with a third approximately decoupled right-handed neutrino provides a close approximation to this situation. Therefore in both cases, observation of leptonic CP violation in low energy neutrino oscillation experiments is directly linked to cosmological CP violation, which both vanish in the same limit.

⁴Note that CSD(4), when implemented in unified models with $Y^u = Y^\nu$, with the second column proportional to $(1, 4, 2)$, predicts a Cabibbo angle $\theta_C \approx 1/4$ in the diagonal $Y^d \sim Y^e$ basis. Pati-Salam models have been constructed along these lines [18].

⁵An analogous approach based on $\Delta(6N^2)$ has also been considered in the quark sector [24].

One may think of the two input mass parameters $m_a = |a|^2/M_{\text{atm}}$ and $m_b = |b|^2/M_{\text{sol}}$ as being used to fix the two experimental mass squared differences. The entire PMNS mixing matrix (three angles and three phases) is then determined by one input phase $\eta = \arg(b^2/a^2)$. *A priori* there is no reason to expect one input parameter η to yield an accurate fit to the three leptonic angles. However we find excellent fits for CSD(3) and CSD(4), with favoured values of η near $2\pi/3$ and $4\pi/5$, respectively, consistent with spontaneous CP violation of an Abelian symmetry Z_{3N} or Z_{5N} symmetry, as previously observed [16, 17]. Unlike these earlier studies, however, here we perform a global fit leading to more robust results which allow the input phase to be determined from the data on the mixing angles. Indeed it is reassuring to see the remarkably simple rational values of the input phase $2\pi/3$ or $4\pi/5$ emerge from the global fit.

From the point of view of discrete family symmetry models, CSD(n) corresponds to the flavon field ϕ_{sol} associated with the solar neutrino gaining a vacuum expectation value (VEV) alignment proportional to $(1, n, n - 2)$, while the atmospheric neutrino flavon ϕ_{atm} has a VEV alignment proportional to $(0, 1, 1)$. In an Appendix we shall discuss a generic flavour model framework, based on A_4 family symmetry, where such vacuum alignments arise due to orthogonality conditions. In such a framework it is natural to expect also alignments such as $(0, 0, 1)$ to also play a role. We shall consider the effect of a third almost decoupled right-handed neutrino involving ϕ_{dec} with a vacuum alignment $(0, 0, 1)$, which introduces a further mass parameter m_c and relative phase ξ , in order to gauge the effect of having a non-zero lightest neutrino mass m_1 . For low values of m_c , this provides a perturbation to our previous results leading to an upper limit on the lightest physical neutrino mass $m_1 \lesssim 1$ meV for the viable cases.

The remainder of the paper is set out as follows. Section 2 defines the see-saw conventions and gives the CSD(n) neutrino mass matrices. In Section 3 we define a test-statistic χ^2 and outline the method for finding and evaluating the global minima in parameter space. In Section 4 we present the results of our χ^2 analysis, first for the case of two right-handed neutrinos, then with three right-handed neutrinos, plotting the results against both n and the mass of the lightest neutrino m_1 , for two choices of relative phase between submatrices of the neutrino mass matrix. In subsection 4.3 we consider particular phase choices for CSD(3) and CSD(4), prompted by the results of our fit and specific model considerations. In Section 5 we discuss the link between the oscillation phase δ_{CP} and leptogenesis in CSD(n). Section 6 concludes the paper. Appendix A shows how CSD(n) can be achieved in a generic model based on A_4 family symmetry, while Appendix B discusses in more detail the χ^2 distribution of the parameters.

2. See-saw conventions and CSD(n) mass matrices

The charged lepton and neutrino Yukawa matrices Y^e , Y^ν are defined in a LR convention by⁶

$$\mathcal{L}^{LR} = -H^d Y_{ij}^e \bar{L}_L^i e_R^j - H^u Y_{ij}^\nu \bar{L}_L^i \nu_R^j + \text{h.c.} \quad (2.1)$$

where $i, j = 1, 2, 3$ label the three families of lepton doublets L_i , right-handed charged leptons e_R^j and right-handed neutrinos ν_R^j ; H^u , H^d are the electroweak Higgs doublets which develop VEVs v_u, v_d . The physical effective neutrino Majorana mass matrix m^ν is determined from the columns of Y^ν via the see-saw mechanism,

$$m^\nu = v_u^2 Y^\nu M_{RR}^{-1} Y^{\nu T} \quad (2.2)$$

where the light Majorana neutrino mass matrix m^ν is defined⁷ by $\mathcal{L}_\nu^{LL} = -\frac{1}{2} m^\nu \bar{\nu}_L \nu_L^c + \text{h.c.}$, while the heavy right-handed Majorana neutrino mass matrix M_R is defined by $\mathcal{L}_\nu^{RR} = -\frac{1}{2} M_{RR} \bar{\nu}_R^c \nu_R + \text{h.c.}$.

In the above conventions, the CSD(n) mass matrices are defined as in Eqs. 1.4, 1.5,

$$m^D = Y^\nu v_u = \begin{pmatrix} 0 & b & 0 \\ a & nb & 0 \\ a & (n-2)b & c \end{pmatrix}, \quad M_R = \begin{pmatrix} M_{\text{atm}} & 0 & 0 \\ 0 & M_{\text{sol}} & 0 \\ 0 & 0 & M_{\text{dec}} \end{pmatrix}. \quad (2.3)$$

Applying the see-saw in Eq. 1.1 for these matrices gives a light neutrino mass matrix,

$$m_{(n)}^\nu = m_a e^{i\alpha} \begin{pmatrix} 0 & 0 & 0 \\ 0 & 1 & 1 \\ 0 & 1 & 1 \end{pmatrix} + m_b e^{i\beta} \begin{pmatrix} 1 & n & n-2 \\ n & n^2 & n(n-2) \\ n-2 & n(n-2) & (n-2)^2 \end{pmatrix} + m_c e^{i\gamma} \begin{pmatrix} 0 & 0 & 0 \\ 0 & 0 & 0 \\ 0 & 0 & 1 \end{pmatrix} \quad (2.4)$$

where $m_a = |a|^2/M_{\text{atm}}$, $m_b = |b|^2/M_{\text{sol}}$ and $m_c = |c|^2/M_{\text{dec}}$ are real and positive combinations of other physical parameters, with the phases displayed explicitly as $\alpha = \arg(a^2)$, $\beta = \arg(b^2)$ and $\gamma = \arg(c^2)$. An overall unphysical phase α may be factored out and then dropped in order to make the term proportional to m_a is real, wherein we make the redefinitions $\eta = \beta - \alpha$ and $\xi = \gamma - \alpha$. Hence $\eta = \arg(b^2/a^2)$ and $\xi = \arg(c^2/a^2)$.

The neutrino mass matrix m^ν is diagonalised by

$$U_{\nu_L} m^\nu U_{\nu_L}^T = \begin{pmatrix} m_1 & 0 & 0 \\ 0 & m_2 & 0 \\ 0 & 0 & m_3 \end{pmatrix}. \quad (2.5)$$

⁶This LR convention for the Yukawa matrix differs by an Hermitian conjugation compared to that used in the MPT package [25] due to the RL convention used there.

⁷Note that this convention for the light effective Majorana neutrino mass matrix m^ν differs by an overall complex conjugation compared to that used in the MPT package [25].

The PMNS matrix is then given by $U_{\text{PMNS}} = U_{e_L} U_{\nu_L}^\dagger$, where U_{e_L} is given by

$$U_{e_L} Y^e U_{e_R}^\dagger = \begin{pmatrix} y_e & 0 & 0 \\ 0 & y_\mu & 0 \\ 0 & 0 & y_\tau \end{pmatrix} \quad (2.6)$$

We use the standard PDG parameterization [26] $U_{\text{PMNS}} = R_{23}^l U_{13}^l R_{12}^l P_{\text{PDG}}$ in terms of $s_{ij} = \sin \theta_{ij}$, $c_{ij} = \cos \theta_{ij}$, the Dirac CP violating phase δ_{CP} and further Majorana phases contained in $P_{\text{PDG}} = \text{diag}(1, e^{i\frac{\alpha_{21}}{2}}, e^{i\frac{\alpha_{31}}{2}})$. We shall assume that Y^e is diagonal, hence U_{e_L} is the identity matrix up to diagonal phase rotations, and that $U_{\text{PMNS}} = U_{\nu_L}^\dagger$, i.e. simply the matrix that diagonalises the neutrino mass matrix, up to charged lepton phase rotations. Appendix A shows how a diagonal charged lepton Yukawa matrix and a neutrino Yukawa matrix with CSD(n) structure can be achieved in a generic model based on A_4 family symmetry.

3. The χ^2 test

3.1. Definition

We define a function χ^2 to serve as a test-statistic for the goodness-of-fit of a chosen vector $x = (m_a, m_b, m_c, \eta, \xi)$ in input parameter space in analogy to [27],

$$\chi^2 = \sum_{i=1}^5 \left(\frac{P_i(x) - \mu_i}{\sigma_i} \right)^2 \quad (3.1)$$

where μ_i are the current experimental best-fit values and σ_i are the 1σ spreads for each of the five physical predictions P_i made, i.e. for the (squared sines of) three PMNS mixing angles θ_{ij} and two mass-squared differences Δm_{21}^2 and Δm_{31}^2 . For definiteness, all data is taken from just one of the global fits, namely that in [2], which is reproduced in Table 1 for the case of a normal mass squared ordering predicted by CSD(n) models. Bounds exist for the CP-violating phase δ_{CP} at 1σ , but it is completely undetermined at 3σ , and so is left as a pure prediction, as are the two Majorana phases.

The meaning of χ^2 in our fit can be understood by calculating χ^2 with each P_i chosen to be $+1\sigma$ away from the experimental best-fit value which yields $\chi^2 \approx 1.05$. Thus we make the generic statement that $\chi^2 \lesssim 1$ is heuristically equivalent to a better-than- 1σ fit. Similarly if we were to choose each P_i to be $+3\sigma$ away from its mean for each variable we would find $\chi^2 \approx 16.5$. While the first case would seem quite likely, the second case would seem to be extremely unlikely. Therefore we regard $\chi^2 \lesssim 1$ as an excellent fit, with $\chi^2 \gtrsim 10$ corresponding to a poor fit, with anything in between as more or less acceptable.

| | bfp $\pm 1\sigma$ | 3σ range |
|--|------------------------------|-----------------------------|
| $\sin^2 \theta_{12}$ | $0.304^{+0.013}_{-0.012}$ | $0.270 \rightarrow 0.344$ |
| $\theta_{12} (^\circ)$ | $33.48^{+0.78}_{-0.75}$ | $31.29 \rightarrow 35.91$ |
| $\sin^2 \theta_{23}$ | $0.452^{+0.052}_{-0.028}$ | $0.382 \rightarrow 0.643$ |
| $\theta_{23} (^\circ)$ | $42.3^{+3.0}_{-1.6}$ | $38.2 \rightarrow 53.3$ |
| $\sin^2 \theta_{13}$ | $0.0218^{+0.0010}_{-0.0010}$ | $0.0186 \rightarrow 0.0250$ |
| $\theta_{13} (^\circ)$ | $8.5^{+0.20}_{-0.21}$ | $7.85 \rightarrow 9.10$ |
| $\delta_{CP} (^\circ)$ | 306^{+39}_{-70} | $0 \rightarrow 360$ |
| $\frac{\Delta m_{21}^2}{10^{-5}} \text{ eV}^2$ | $7.50^{+0.19}_{-0.17}$ | $7.02 \rightarrow 8.09$ |
| $\frac{\Delta m_{31}^2}{10^{-3}} \text{ eV}^2$ | $+2.457^{+0.047}_{-0.047}$ | $+2.317 \rightarrow +2.607$ |

Table 1: Table of current best fits to experimental data for neutrino mixing angles and masses case of normal mass squared ordering taken from [2], with 1σ and 3σ uncertainty ranges. These are the values that we use in the CSD(n) fits, apart from δ_{CP} which we leave as an unconstrained output prediction since its non-zero value has not yet been firmly established experimentally.

3.2. Minimising method

Initially, a coarse Monte-Carlo was used to examine the (5-dimensional) parameter space. A random vector $(m_a, m_b, m_c, \eta, \xi)$ is chosen, all PMNS parameters are calculated numerically using the Mixing Parameter Tools (MPT) package for Mathematica [28], and χ^2 is evaluated. A large- N search of this type reveals the existence of two collections of global minima. These regions in parameter space are characterised by having the same approximate values of m_a and m_b , while m_c and ξ are allowed to take a broad range of values (in fact ξ can take any value at all in $[-\pi, \pi]$).

Meanwhile η is constrained only up to a sign – the two minima then correspond to equal and opposite values of η . Refining the input parameter space by allowing only $\eta \in (0, \pi)$ leaves a single global minimum region. This minimum is well-defined and generally stable, meaning our χ^2 statistic is a good test for goodness-of-fit over this space; this is true for all CSD(n). For more details on the behaviour of χ^2 near the global minimum, see Appendix B.

4. Results

This section details results for the properties of general CSD(n) vacuum alignments, wherein we have simplified the analysis by considering only two planes of fixed ξ , i.e. the cases where $\xi = 0$ (phase aligned with dominant mass matrix) or $\xi = \eta$ (phase aligned with subdominant mass matrix). This simplification is predicated on the underlying assumption from CSD that the contribution from the m_c term in Eq. 2.2 is small; indeed, a stable minimum of the same order in χ^2 can be found for any value of ξ . Such a constraint on ξ may also arise directly from a model, such as in [18].

In all subsequent plots, a thick solid gridline corresponds to a best-fit value of a mixing angle or neutrino mass, while thin solid gridlines show the 1σ limits, and thin dashed gridlines show the 3σ range.

4.1. CSD(n) with two right-handed neutrinos

Models with only two right-handed neutrinos are compelling as they are typically highly predictive. In a CSD(n) framework, the neutrino mass matrix in Eq. 2.4 simplifies in the two right-handed neutrino case to

$$m_{(n)}^\nu = m_a \begin{pmatrix} 0 & 0 & 0 \\ 0 & 1 & 1 \\ 0 & 1 & 1 \end{pmatrix} + m_b e^{i\eta} \begin{pmatrix} 1 & n & n-2 \\ n & n^2 & n(n-2) \\ n-2 & n(n-2) & (n-2)^2 \end{pmatrix}, \quad (4.1)$$

where we have defined $\eta = \beta - \alpha$ and removed an overall unphysical phase α . This case immediately predicts the lightest physical neutrino mass to be zero, $m_1 = 0$. For a given choice of alignment n , there are three real input parameters m_a , m_b and η from which two light physical neutrino masses m_2 , m_3 , three lepton mixing angles, the CP-violating phase δ_{CP} and two Majorana phases are derived; a total of nine physical parameters from three input parameters, i.e. six predictions for each value of n . As the Majorana phases are not known and δ_{CP} is only tentatively constrained by experiment, this leaves five presently measured observables, namely the two neutrino mass squared differences and the three lepton mixing angles, from only three input parameters.

Table 2 shows all fitted parameters with respect to n . Fig. 2 shows the best-fit values of χ^2 with respect to vacuum alignment n . Only CSD(3) and CSD(4) pass the requirement for a better-than- 1σ fit, defined in this analysis as $\chi^2 \lesssim 1$. Indeed, given the predictivity of a two-neutrino model, the CSD(3) and CSD(4) fits are remarkable. In Fig. 3 and Fig. 4 we show the variation of physical masses and neutrino mixing angles with respect to n in the two right-handed neutrino CSD(n) model. Note that, in our conventions defined earlier, a positive value of η , namely $\eta \in (0, \pi)$, yields a negative CP-violating angle, i.e. $\delta_{CP} \in (0, -\pi)$, while the mirror global minimum for $\eta \in (-\pi, 0)$ corresponds uniquely to $\delta_{CP} \in (\pi, 0)$. As η is unconstrained (unless some model explicitly restricts

| n | m_a (meV) | m_b (meV) | η (rad) | θ_{12} ($^\circ$) | θ_{13} ($^\circ$) | θ_{23} ($^\circ$) | $ \delta_{CP} $ ($^\circ$) | m_2 (meV) | m_3 (meV) | χ^2 |
|-----|----------------|----------------|-----------------|-------------------------------|-------------------------------|-------------------------------|---------------------------------|----------------|----------------|----------|
| 1 | 24.8 | 2.89 | 1.46 | 35.3 | 0 | 45.0 | 0 | 8.66 | 49.6 | 121 |
| 2 | 19.6 | 3.68 | 0 | 34.5 | 7.74 | 56.1 | 0 | 8.89 | 48.6 | 14.8 |
| 3 | 27.2 | 2.63 | 2.16 | 34.4 | 8.45 | 44.7 | 91.2 | 8.67 | 49.5 | 0.717 |
| 4 | 36.9 | 1.94 | 2.66 | 34.3 | 8.63 | 37.9 | 123 | 8.63 | 49.7 | 1.41 |
| 5 | 46.8 | 1.52 | 3.01 | 34.3 | 8.83 | 33.0 | 160 | 8.59 | 49.8 | 5.10 |
| 6 | 55.0 | 1.29 | 3.14 | 34.2 | 9.31 | 31.6 | 180 | 8.47 | 50.2 | 11.2 |
| 7 | 63.0 | 1.12 | 3.14 | 34.1 | 9.70 | 31.0 | 180 | 8.36 | 50.5 | 19.4 |
| 8 | 71.0 | 0.986 | 3.14 | 34.0 | 9.98 | 30.6 | 180 | 8.27 | 50.8 | 27.8 |
| 9 | 79.0 | 0.880 | 3.14 | 33.9 | 10.2 | 30.3 | 180 | 8.19 | 50.9 | 35.7 |

Table 2: Table of best-fit parameters for two right-handed neutrino CSD(n) model for $1 \leq n \leq 9$. The fitted three input parameters m_a , m_b and η yield nine physical predictions, but only six physical outputs are shown. The undisplayed outputs are $m_1 = 0$ in each case and the two Majorana phases which are difficult to measure for a normal hierarchy.

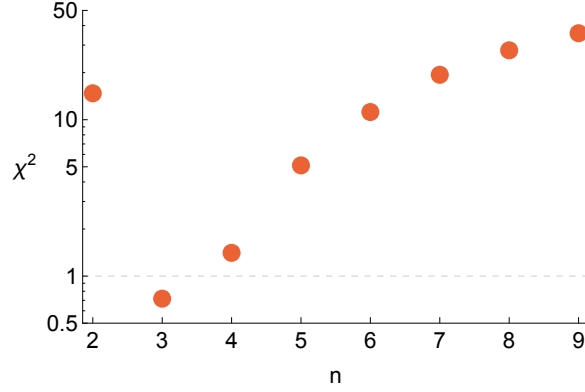


Fig. 2: Best-fit χ^2 variation with respect to n . The horizontal gridline at $\chi^2 \sim 1$ marks the approximate boundary of a roughly 1σ fit.

its domain), only the absolute value of δ_{CP} can be predicted by this analysis. In Table 2 we only show positive η values, for which δ_{CP} is negative.

Roughly speaking the two input masses m_a , m_b fix the two light neutrino masses m_2 , m_3 after which the entire PMNS matrix is determined from only one parameter, namely the phase η . *A priori*, CSD(n) has no right to work for any value of n , and yet the results show that it gives remarkably good fits to the leptonic mixing angles for $n = 3, 4$, yielding a value of $|\delta_{CP}|$ (which is taken to be unconstrained by data) as a genuine prediction, along with preferred values for the lepton angles.

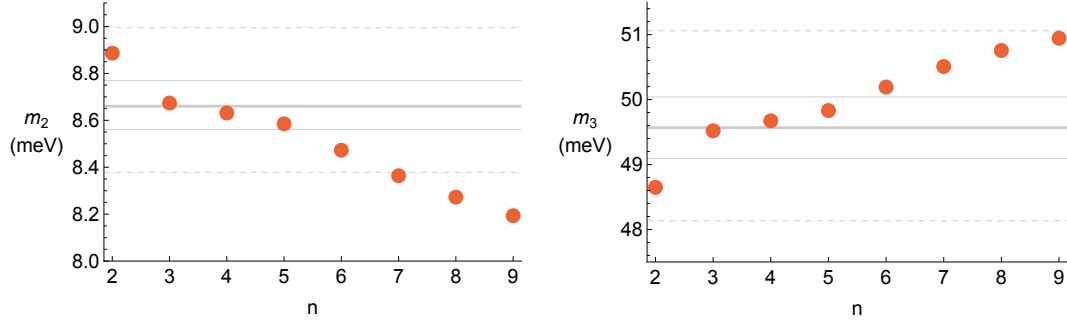


Fig. 3: Best-fit light neutrino masses with respect n , for the two right-handed neutrino CSD(n) model. Since $m_1 = 0$ in this case $m_2 = \sqrt{\Delta m_{21}^2}$ and $m_3 = \sqrt{\Delta m_{31}^2}$.

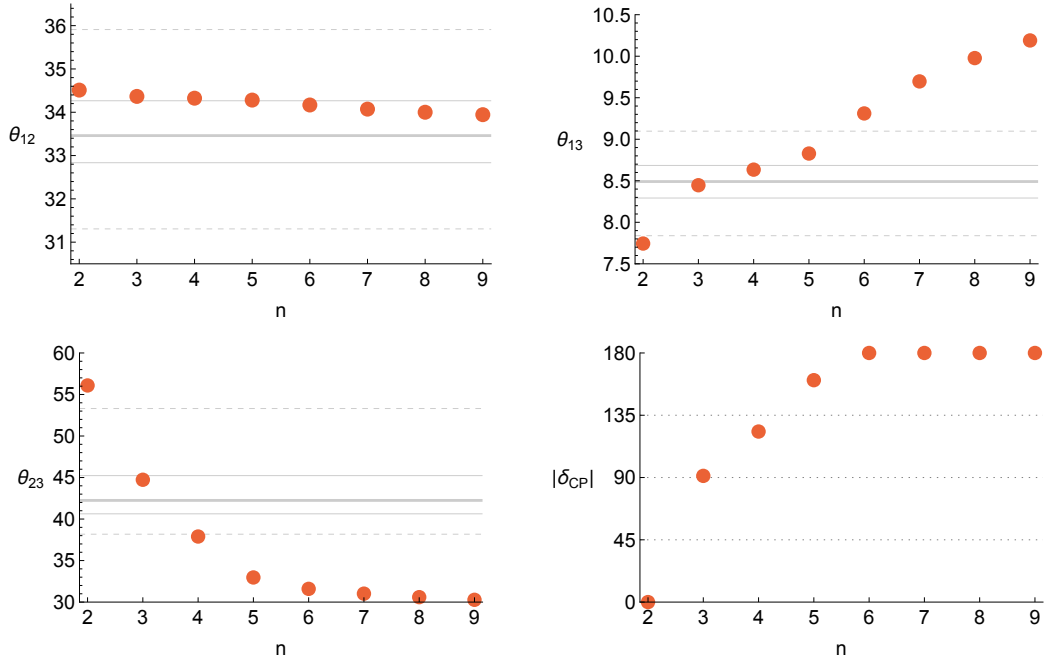


Fig. 4: Best-fit PMNS mixing angles and CP-violating phase with respect to n , for the two right-handed neutrino CSD(n) model. We emphasise that $|\delta_{CP}|$ is a genuine prediction here since we have not used the one sigma hint from experiment as an input constraint. It is striking that both CSD(3) and CSD(4) both yield predictions within the preferred range $|\delta_{CP}| \sim 90^\circ \pm 45^\circ$ but may be distinguished by their differing predictions for the atmospheric angle $\theta_{23} \approx 45^\circ$ and $\theta_{23} \approx 38^\circ$, respectively.

4.2. CSD(n) with three right-handed neutrinos

We now extend the analysis to the case of three right-handed neutrinos,

$$m_{(n)}^\nu = m_a \begin{pmatrix} 0 & 0 & 0 \\ 0 & 1 & 1 \\ 0 & 1 & 1 \end{pmatrix} + m_b e^{i\eta} \begin{pmatrix} 1 & n & n-2 \\ n & n^2 & n(n-2) \\ n-2 & n(n-2) & (n-2)^2 \end{pmatrix} + m_c e^{i\xi} \begin{pmatrix} 0 & 0 & 0 \\ 0 & 0 & 0 \\ 0 & 0 & 1 \end{pmatrix} \quad (4.2)$$

where the overall unphysical phase α in Eq. 2.4 has been factored out and dropped. The immediate effect of including a third right-handed neutrino is to switch on a non-zero value for the lightest physical neutrino mass m_1 , where previously for the case of two right-handed neutrinos we had $m_1 = 0$.

Since the contribution from the “decoupled” right-handed neutrino is assumed to be a perturbation to the case of two right-handed neutrinos considered in the previous subsection, the detailed structure of the third matrix is irrelevant, and it is sufficient to only keep the most important term in the third matrix, which we have assumed to be in the (3,3) entry, since in unified models where $Y^u = Y^\nu$ this entry is responsible for the top quark Yukawa coupling [18]. However the third term brings in a further undetermined relative phase ξ which complicates the analysis somewhat. Since the results are not sensitive to this phase ξ we have taken the approach of fixing it to take two simple values, namely $\xi = 0$ and $\xi = \eta$, in order to illustrate the sensitivity of the results to this phase without over-complicating the analysis. These two examples also correspond to the values appearing in certain realistic models [18].

Once the existence of a single stable minimum has been confirmed⁸, Tables 3 and 4 show the results for the best fit or optimal χ^2 and its corresponding input and output values, for CSD(n) with $1 \leq n \leq 9$, for each of the two sub-subdominant phases considered, i.e. $\xi = 0$ and $\xi = \eta$. As in the two right-handed neutrino case, CSD(3) easily satisfies the one sigma condition $\chi^2 \lesssim 1$. Also CSD(4) can achieve $\chi^2 \lesssim 1$, with a best-fit value of 0.940(0.787), for $\xi = 0$ ($\xi = \eta$).

As n increases, the global fit prefers a stronger hierarchy of input neutrino masses m_a and m_b , while the contribution from m_c becomes stronger. The fits select the input mass parameters m_a , m_b and m_c which are allowed to be free apart from an upper limit imposed on $m_c < 10$ meV in order not to violate the condition of sequential dominance as discussed in the Introduction. In the case of $\xi = 0$, m_c reaches the upper bound of 10 meV for CSD($n \geq 7$).⁹ However for the successful cases CSD(3) and CSD(4), the best fit value of m_c are comfortably below 10 meV, so these cases naturally prefer a quite decoupled third right-handed neutrino for which the upper limit of m_c is irrelevant.

⁸This analysis was done using the default minimising algorithms in Mathematica.

⁹Note that a fit that requires a large m_c is not CSD. For example, a proper analysis of such a non-CSD model necessarily includes contributions from elements of the sub-subdominant mass matrix other than the largest (3,3) element, which have been neglected thus far. This would destroy the

| n | m_a (meV) | m_b (meV) | m_c (meV) | η (rad) | θ_{12} ($^\circ$) | θ_{13} ($^\circ$) | θ_{23} ($^\circ$) | $ \delta_{CP} $ ($^\circ$) | m_1 (meV) | m_2 (meV) | m_3 (meV) | χ^2 |
|-----|----------------|----------------|----------------|-----------------|-------------------------------|-------------------------------|-------------------------------|---------------------------------|----------------|----------------|----------------|----------|
| 1 | 22.3 | 2.87 | 8.93 | 1.81 | 33.5 | 0.462 | 39.4 | 247 | 1.32 | 8.76 | 49.6 | 118 |
| 2 | 19.6 | 3.68 | 0 | 0 | 34.5 | 7.74 | 56.1 | 0 | 0 | 8.89 | 48.6 | 14.8 |
| 3 | 25.8 | 2.61 | 1.75 | 2.08 | 33.5 | 8.43 | 44.8 | 80.3 | 0.276 | 8.68 | 49.5 | 0.353 |
| 4 | 32.5 | 1.92 | 5.00 | 2.50 | 33.2 | 8.62 | 38.1 | 90.6 | 0.727 | 8.66 | 49.7 | 0.940 |
| 5 | 38.7 | 1.51 | 7.88 | 2.68 | 32.8 | 8.75 | 34.1 | 92.2 | 1.07 | 8.67 | 49.8 | 3.74 |
| 6 | 44.8 | 1.24 | 9.98 | 2.79 | 32.5 | 8.83 | 31.4 | 92.6 | 1.28 | 8.68 | 49.8 | 6.52 |
| 7 | 51.7 | 1.06 | 10 | 2.84 | 32.2 | 9.12 | 31.1 | 93.1 | 1.27 | 8.62 | 50.0 | 9.43 |
| 8 | 58.5 | 0.928 | 10 | 2.87 | 31.9 | 9.32 | 31.0 | 92.9 | 1.26 | 8.57 | 50.1 | 12.5 |
| 9 | 65.3 | 0.823 | 10 | 2.90 | 31.7 | 9.47 | 31.0 | 92.4 | 1.26 | 8.53 | 50.1 | 15.4 |

Table 3: Table of best-fit parameters for CSD(n) for $1 \leq n \leq 9$ and $\xi = 0$.

| n | m_a (meV) | m_b (meV) | m_c (meV) | η (rad) | θ_{12} ($^\circ$) | θ_{13} ($^\circ$) | θ_{23} ($^\circ$) | $ \delta_{CP} $ ($^\circ$) | m_1 (meV) | m_2 (meV) | m_3 (meV) | χ^2 |
|-----|----------------|----------------|----------------|-----------------|-------------------------------|-------------------------------|-------------------------------|---------------------------------|----------------|----------------|----------------|----------|
| 1 | 24.5 | 2.75 | 1.21 | 0 | 33.4 | 0.067 | 44.2 | 180 | 0.189 | 8.66 | 49.6 | 119 |
| 2 | 19.6 | 3.68 | 0 | 0 | 34.5 | 7.74 | 56.1 | 0.0013 | 0 | 8.89 | 48.6 | 14.8 |
| 3 | 27.1 | 2.62 | 0.653 | 2.14 | 33.6 | 8.43 | 45.1 | 91.7 | 0.108 | 8.68 | 49.5 | 0.428 |
| 4 | 37.1 | 1.91 | 1.15 | 2.66 | 33.2 | 8.60 | 38.5 | 125 | 0.190 | 8.64 | 49.7 | 0.787 |
| 5 | 47.3 | 1.50 | 1.49 | 3.05 | 32.9 | 8.77 | 33.7 | 167 | 0.247 | 8.60 | 49.8 | 4.08 |
| 6 | 55.3 | 1.28 | 1.57 | 3.14 | 32.7 | 9.30 | 32.7 | 180 | 0.261 | 8.47 | 50.2 | 10.2 |
| 7 | 63.3 | 1.11 | 1.50 | 3.14 | 32.7 | 9.69 | 32.1 | 180 | 0.249 | 8.35 | 50.5 | 18.6 |
| 8 | 71.3 | 0.979 | 1.31 | 3.14 | 32.8 | 9.97 | 31.5 | 180 | 0.217 | 8.26 | 50.8 | 27.3 |
| 9 | 79.2 | 0.876 | 1.03 | 3.14 | 33.0 | 10.2 | 31.0 | 180 | 0.171 | 8.18 | 51.0 | 35.3 |

Table 4: Table of best-fit parameters for CSD(n) for $1 \leq n \leq 9$ and $\xi = \eta$.

Among physical parameters, of particular note is the CP-violating phase $|\delta_{CP}|$, which is close to 90° for CSD(3) for both choices of ξ . Furthermore, the alignment of ξ with the dominant or subdominant mass matrix appears to greatly affect the best fit for δ_{CP} . The most likely source of this behaviour is a close relationship between η and δ_{CP} . Notice that when $\xi = \eta$, the best fit of both is 180° for $n \geq 6$.

In Fig. 5 and Fig. 6 we display the variation of the best fit physical parameters – mixing angles and neutrino masses – as a function of n . In Fig. 5 we see that the reactor angle increases with n while the atmospheric and solar angles decrease. Examining the 3σ ranges (dashed lines) we also see that θ_{23} is typically worst fit (only CSD(3) lies within the 1σ bounds), and is also least sensitive to the choice of sub-subdominant phase ξ , which can otherwise improve the fit of θ_{12} and θ_{13} at large n .

The best fit values of m_1 in Fig. 6 indicates that it can vary greatly with n for some

predictivity of the scheme which makes CSD(n) so appealing. This justifies imposing the chosen upper bound on m_c .

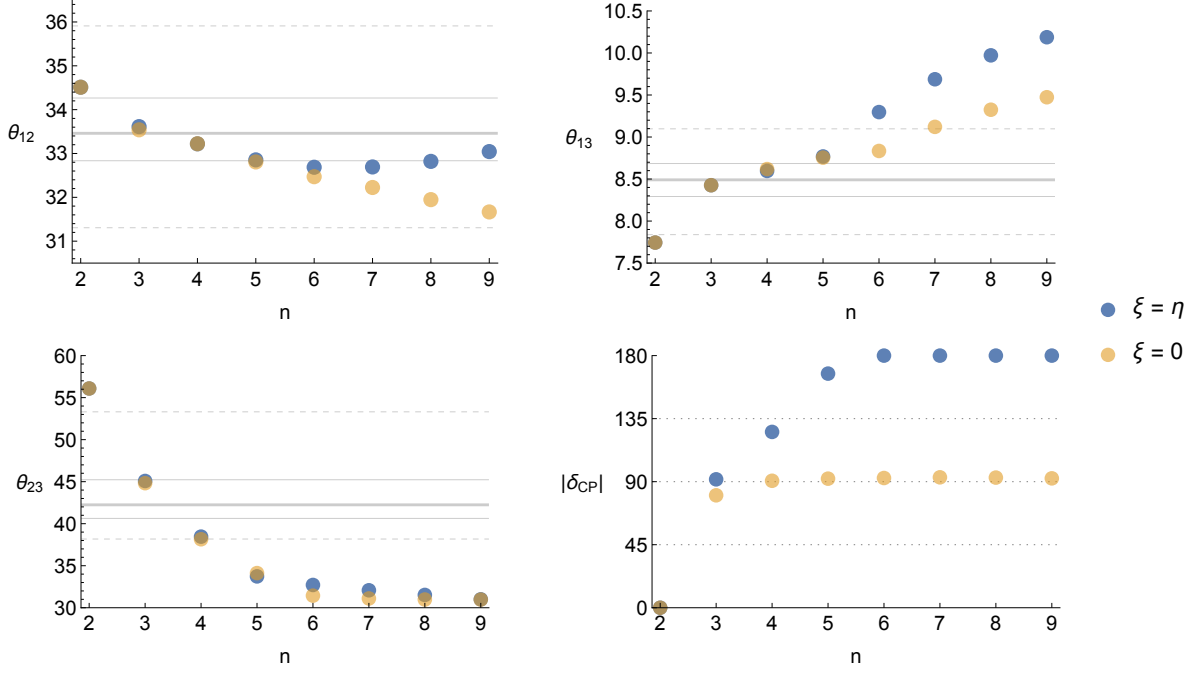


Fig. 5: Best-fit PMNS mixing angles and the CP-violating phase δ_{CP} for CSD(n) with three right-handed neutrinos as a function of n . The cases $\xi = 0$ ($\xi = \eta$) correspond to yellow (blue) dots.

phase choices. It is however unlikely that this can be used to constrain models in the near future, as the mass scale is well below current experimental bounds of $\sum m_\nu < 0.23$ eV [29].

The best fit values of m_1 lie in rather shallow minima of χ^2 as shown in Fig. 7. In Fig. 8 we show the variation of input parameters with lightest neutrino mass m_1 , for the three best fit cases $3 \leq n \leq 5$, while Fig. 9 and 10 show the dependence on m_1 for the predicted mixing angles and neutrino masses, respectively. In all these plots the dashed line is the $\xi = 0$ case, while the solid line is the $\xi = \eta$ case.

We observe that the choice of sub-subdominant phase ξ has a small effect on the value of the global minimum, but can noticeably shift its location in parameter space. Naturally the largest effect is on the best-fit value of m_e , but it also contributes to interference between the three mass matrices in Eq. 2.4. The practical effect is that each of the three vacuum alignments contribute in varying amounts to each of the three PMNS mixing angles depending on the relative phase between the matrices, which can be seen particularly in Fig. 9, where the choice of ξ alters the shape of the variation of the mixing angles. The physical neutrino masses in Fig. 10 are comparatively less sensitive to changes in ξ .

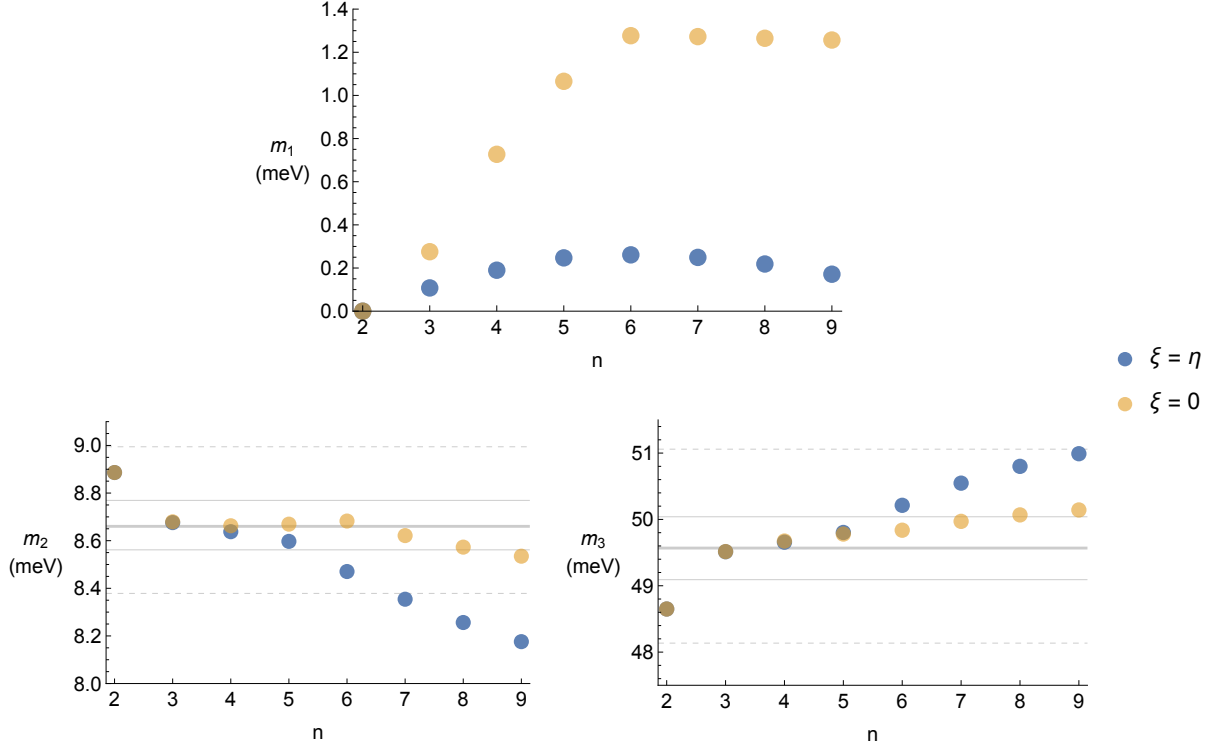


Fig. 6: Best-fit light neutrino masses for $\text{CSD}(n)$ with three right-handed neutrinos as a function of n . The horizontal lines drawn assume m_1 is negligible, such that $m_2 \simeq \sqrt{\Delta m_{21}^2}$ and $m_3 \simeq \sqrt{\Delta m_{31}^2}$. The cases $\xi = 0$ ($\xi = \eta$) correspond to yellow (blue) dots.

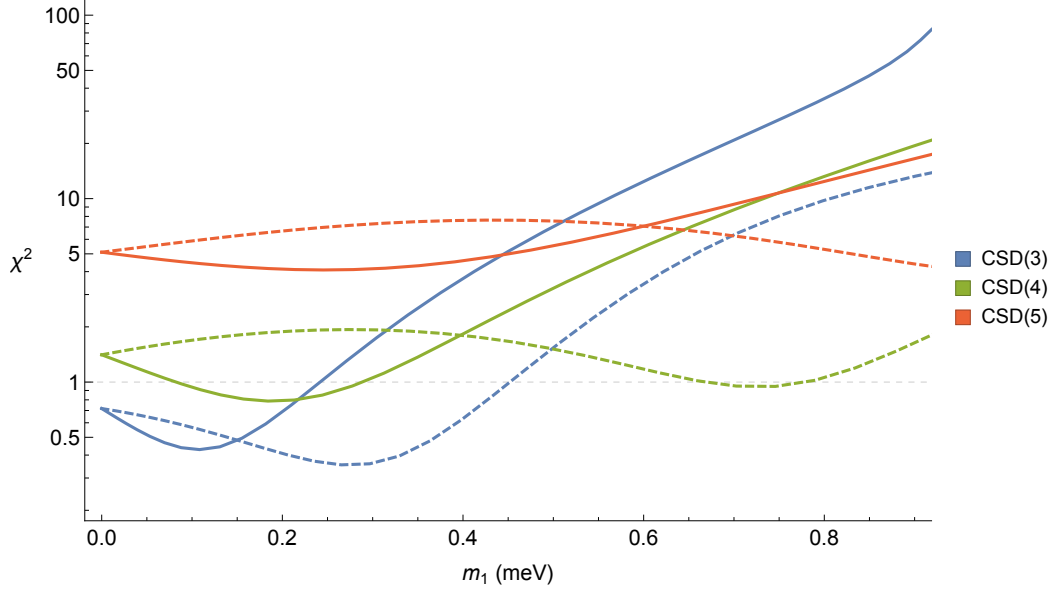


Fig. 7: Goodness-of-fit statistic χ^2 plotted with respect to the lightest neutrino mass m_1 . Note that CSD(3) and CSD(4) have minima at $\chi^2 \lesssim 1$, corresponding loosely to a better-than- 1σ fit, for slightly different values of m_1 . The dashed lines refer to the $\xi = 0$ case, while the solid lines refer to the $\xi = \eta$ case.

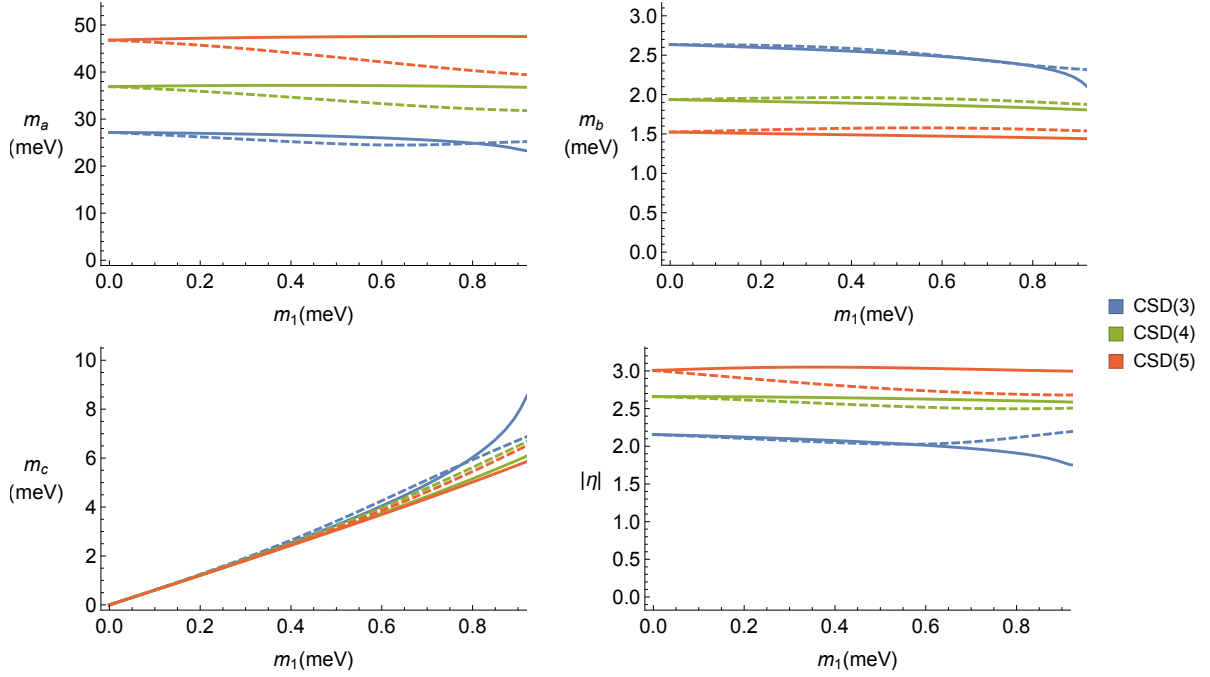


Fig. 8: The variation with m_1 of the best-fit input parameters. Note that m_c and m_1 are closely correlated. The dashed lines refer to the $\xi = 0$ case, while the solid lines refer to the $\xi = \eta$ case.

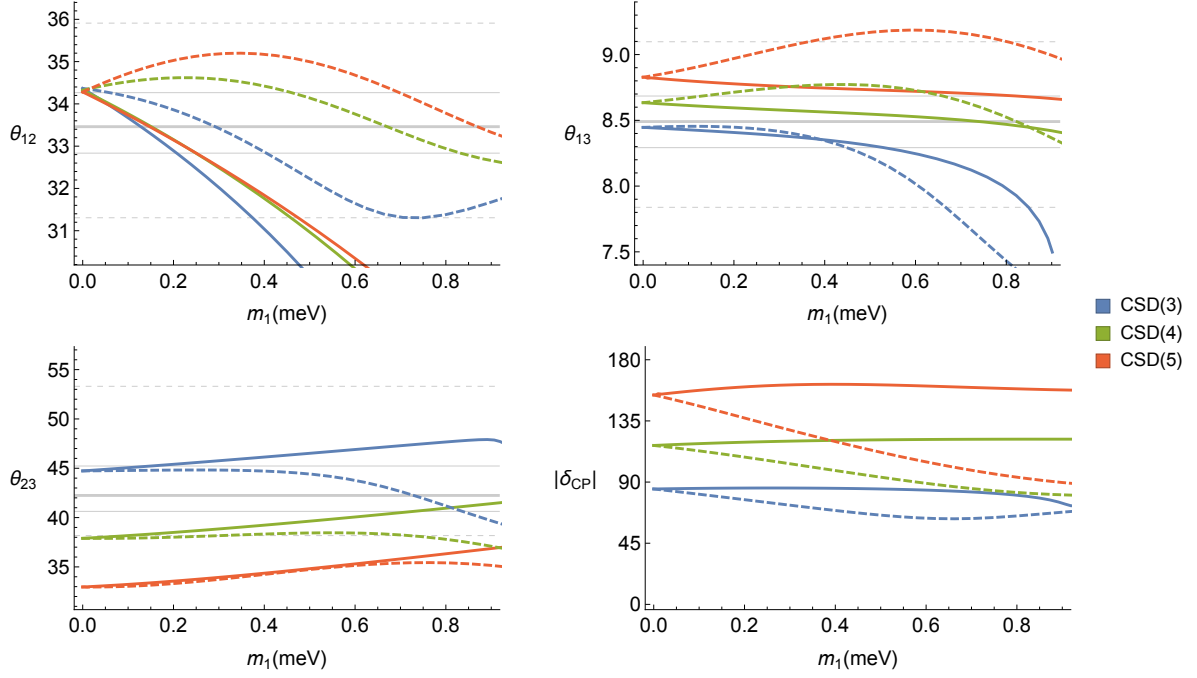


Fig. 9: Predicted best fit mixing angles and the CP-violating phase plotted with respect to m_1 . Note that the variation is mainly in θ_{12} when m_1 is small. The dashed lines refer to the $\xi = 0$ case, while the solid lines refer to the $\xi = \eta$ case.

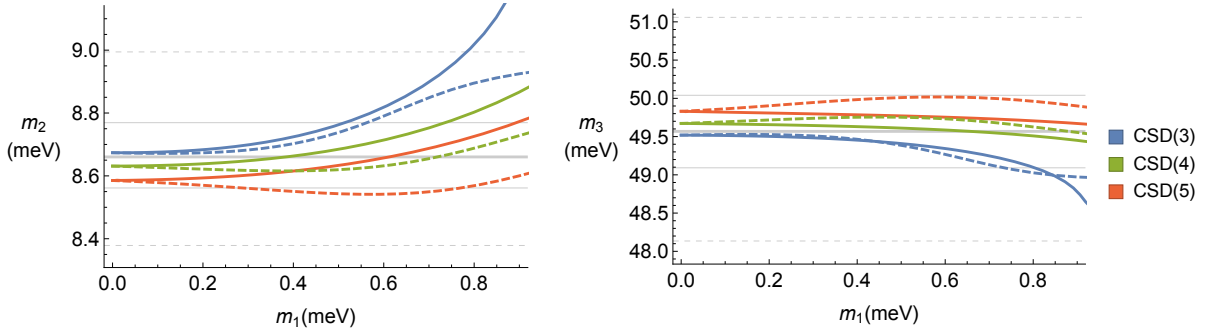


Fig. 10: Second and third best fit neutrino masses plotted with respect to the lightest neutrino mass m_1 . The horizontal gridlines drawn assume m_1 is negligible, such that $m_2 \simeq \sqrt{\Delta m_{21}^2}$ and $m_3 \simeq \sqrt{\Delta m_{31}^2}$. The dashed lines refer to the $\xi = 0$ case, while the solid lines refer to the $\xi = \eta$ case.

4.3. CSD(3) with $\eta = 2\pi/3$ and CSD(4) with $\eta = 4\pi/5$

It is interesting that the optimal fit for the CSD(3) with $\chi^2 = 0.353(0.428)$ corresponds to a choice of input phase $|\eta| = 2.08(2.14) = 0.662\pi(0.681\pi)$, for the $\xi = 0$ ($\xi = \eta$) cases, respectively. Its closeness to the value $2\pi/3$, independently of ξ , is a compelling quality in favour of flavour models that predict additional Z_{3N} symmetries, which tend to predict quantised phases as multiples of $\pi/3$. This motivates a χ^2 analysis with a fixed value of $\eta = 2\pi/3$, for a reduced input vector $x = (m_a, m_b, m_c)$. The resulting input and output parameters for fixed $\eta = 2\pi/3$ are given in Table 5. The best fits give $\chi^2 = 0.362(0.678)$, for the $\xi = 0$ ($\xi = \eta$) cases, respectively, slightly worse than in the case of unconstrained η fits which gave $\chi^2 = 0.353(0.428)$, but still satisfying $\chi^2 \lesssim 1$.

Turning to the other promising candidate, CSD(4), we see that, for $\xi = 0$ ($\xi = \eta$), we have $\chi^2 = 0.940(0.787)$ for $|\eta| = 2.50(2.66) = 0.80\pi(0.85\pi)$, which is close to $4\pi/5$. Based on the work in [18], it is meaningful to examine the parameter space for a fixed phase $\eta = \pm\frac{4\pi}{5}$ and $\xi = 0$ or $\xi = \eta$.¹⁰ χ^2 -minimisation yields $\chi^2 = 0.964(3.62)$ with corresponding input and output parameters given in Table 6. The case with $\xi = 0$ gives the best fit with $\chi^2 \sim 1$.

| | | $\xi = 0$ | $\xi = \eta$ |
|--------|----------------------------|-----------|--------------|
| Input | m_a (meV) | 26.0 | 26.7 |
| | m_b (meV) | 2.61 | 2.64 |
| | m_c (meV) | 1.61 | 0.883 |
| Output | m_1 (meV) | 0.261 | 0.145 |
| | m_2 (meV) | 8.70 | 8.63 |
| | m_3 (meV) | 48.3 | 49.7 |
| | θ_{12} ($^\circ$) | 32.3 | 33.3 |
| | θ_{13} ($^\circ$) | 8.74 | 8.55 |
| | θ_{23} ($^\circ$) | 46.1 | 45.8 |
| | δ_{CP} ($^\circ$) | 89.8 | 89.0 |

Table 5: Best-fit input and output values corresponding to $\chi^2 = 0.362(0.678)$ for $\xi = 0$ ($\xi = \eta$) for a CSD(3) with a fixed input phase $\eta = 2\pi/3$.

¹⁰Note that the first paper in [18] involved $\xi = 0$ while the second paper used $\xi = \eta$. However in such realistic models the charged lepton corrections also play a role.

| | | $\xi = 0$ | $\xi = \eta$ |
|--------|----------------------------|-----------|--------------|
| Input | m_a (meV) | 32.8 | 35.3 |
| | m_b (meV) | 1.92 | 1.99 |
| | m_c (meV) | 4.93 | 1.51 |
| Output | m_1 (meV) | 0.722 | 0.250 |
| | m_2 (meV) | 8.67 | 8.50 |
| | m_3 (meV) | 49.7 | 50.1 |
| | θ_{12} ($^\circ$) | 33.4 | 32.7 |
| | θ_{13} ($^\circ$) | 8.60 | 9.07 |
| | θ_{23} ($^\circ$) | 37.9 | 41.3 |
| | δ_{CP} ($^\circ$) | 92.3 | 111 |

Table 6: Best-fit input and output values corresponding to $\chi^2 = 0.964(3.62)$ for $\xi = 0$ ($\xi = \eta$) for a CSD(4) with a fixed input phase $\eta = 4\pi/5$.

5. The link between δ_{CP} and leptogenesis in CSD(n)

Leptogenesis [30] is a leading candidate for the origin of matter-antimatter asymmetry in the universe. In the original form of CSD, the columns of the Dirac mass matrix in the flavour basis were orthogonal to each other and consequently the CP asymmetries for cosmological leptogenesis vanished [31, 32]. Following the subsequent observation that leptogenesis also vanished for a range of other family symmetry models [33], this undesirable feature was eventually understood [34] to be a general consequence of see-saw models with form dominance [14] (i.e. in which the columns of the Dirac mass matrix in the flavour basis are proportional to the columns of the PMNS mixing matrix).

In the case for CSD(n), leptogenesis does not vanish since the columns of the Dirac mass matrix in the flavour basis are not orthogonal. To be precise, $(m_{\text{atm}}^D)^T = (0, a, a)$ and $(m_{\text{sol}}^D)^T = (b, nb, (n-2)b)$ from Eqs. 1.4, 1.5 are not orthogonal for $n > 1$.¹¹ Interestingly, since the see-saw mechanism in CSD(n) with two right-handed neutrinos only involves a single phase $\eta = \arg(b^2/a^2)$, both the leptogenesis asymmetries and the neutrino oscillation phase δ_{CP} must necessarily originate from η , providing a direct link between the two CP violating phenomena in this class of models, as follows.

The produced baryon asymmetry Y_B from leptogenesis in two right-handed neutrino models with CSD(n) satisfies, following the arguments in [31],

$$Y_B \propto \pm \sin \eta, \quad (5.1)$$

where the “+” sign applies to the case $M_{\text{atm}} \ll M_{\text{sol}}$ and the “−” sign holds for the case $M_{\text{sol}} \ll M_{\text{atm}}$. Since the observed baryon asymmetry Y_B is positive, it follows that, for

¹¹Note that the original CSD($n = 1$) case satisfies form dominance since $(0, a, a) \cdot (b, b, -b) = 0$. Hence leptogenesis vanishes in this case. However CSD(1) is excluded due to observed reactor angle and we find $\chi^2 \sim 120$.

$M_{\text{atm}} \ll M_{\text{sol}}$, we must have $\sin \eta$ to be positive, while for $M_{\text{sol}} \ll M_{\text{atm}}$ we must have $\sin \eta$ to be negative. We have seen that for CSD(n) positive η is associated with negative δ_{CP} and *vice versa*. Although the global fits do not distinguish the sign of η , the present hint that $\delta_{CP} \sim -\pi/2$ would require positive η , then in order to achieve positive Y_B we require $M_{\text{atm}} \ll M_{\text{sol}}$, corresponding to “light sequential dominance”, depicted in Fig. 1, as considered in the two right-handed neutrino analysis in [36].

The above link between CP violation in flavour dependent leptogenesis and neutrino oscillation for models with sequential dominance was observed in [31], although with only one leptogenesis phase the conclusions are identical to those obtained in the flavour independent or “vanilla” case [35]. Our discussion here generalises that of CSD(2) which involves two texture zeroes [15]. Here we find a link for CSD(n), even without two texture zeroes, due to the appearance of only a single phase η in the see-saw mechanism, for the case of two right-handed neutrinos, where η is identified as both the leptogenesis phase in Eq. 5.1 and the phase appearing in the neutrino mass matrix in Eq. 4.1.

The above conclusions remain approximately true when a third almost decoupled right-handed neutrino is introduced, as is necessary in the realistic Pati-Salam models based on CSD(4) in [18]. In these models the new phase is either given by $\xi = 0$ or $\xi = \eta$, so no new leptogenesis phase appears. However the mechanism for leptogenesis is necessarily quite different in these models, since the lightest right-handed neutrino of mass M_{atm} is too light to generate successful leptogenesis in its decays. Instead one must rely on the decays of the second lightest right-handed neutrino of mass M_{sol} as in $SO(10)$ -inspired leptogenesis [37]. It would be interesting to discuss this in more detail in a future publication [38].

6. Conclusion

We have performed a global analysis on a class of CSD(n) models in which, in the flavour basis, two right-handed neutrinos are dominantly responsible for the “atmospheric” and “solar” neutrino masses with Yukawa couplings to $(\nu_e, \nu_\mu, \nu_\tau)$ proportional to $(0, 1, 1)$ and $(1, n, n - 2)$, respectively, where n is a positive integer. We have introduced a χ^2 measure which offers a flexible and robust way to examine parameter space for a given form of neutrino mass matrix, and the relative strength of fit to experimental data. The ability to make a direct comparison between a $\chi^2 \sim 1$ value and the 1σ values of the experimental input provides a useful guide to interpreting the results.

With just two right-handed neutrinos, we find excellent agreement with experiment (namely, $\chi^2 \lesssim 1$) for CSD(3) and CSD(4), leading to accurate predictions for mixing angles and the magnitude of the oscillation phase $|\delta_{CP}|$, with these two cases being distinguished by their differing predictions for the atmospheric angle of $\theta_{23} \approx 45^\circ$ and $\theta_{23} \approx 38^\circ$, respectively. We find it truly remarkable that the entire PMNS matrix can

be so accurately fitted in terms of just one input parameter, namely the relative phase η , with the input mass parameters m_a and m_b essentially determining the neutrino mass-squared differences Δm_{21}^2 , Δm_{31}^2 .

We have also carefully studied the perturbing effect of a third “decoupled” right-handed neutrino, leading to a bound on the lightest physical neutrino mass $m_1 \lesssim 1$ meV for the viable cases, corresponding to the robust prediction of a normal neutrino mass hierarchy. The best fit model in this case is shown to be CSD(3), for which we find $\chi^2 = 0.353(0.428)$ with fixed sub-subdominant phase $\xi = 0$ ($\xi = \eta$). CSD(3) has the added desirable property that η is preferred to be close to $2\pi/3$, which can be naturally predicted from flavour models with a Z_{3N} symmetry. Another leading contender is CSD(4) for which we find $\chi^2 = 0.940(0.787)$ with fixed sub-subdominant phase $\xi = 0$ ($\xi = \eta$). For the case $\xi = 0$, CSD(4) prefers η to be close to $4\pi/5$, which can be naturally predicted from flavour models with a Z_{5N} symmetry. However such realistic flavour models will in general also include (small) charged lepton corrections which will modify the fits presented here. CSD(5), although less favoured, provides acceptable fits with $\chi^2 \lesssim 5$.

On the other hand, the present analysis confirms the non-compatibility of CSD(2), as well as disfavouring CSD($n > 5$). Possibilities exist if we allow each physical measurement to within 3σ experimental uncertainty, characterised by $\chi^2 < 16.5$, but such models require tuning of all parameters of the neutrino mass matrix, including relative phases. The analysis is further complicated for larger n by the increasing influence of the sub-subdominant matrix proportional to m_c (which correlates very closely with the lightest neutrino mass). However here we restrict ourselves to the CSD framework where we demand that the third right-handed neutrino be approximately decoupled from the see-saw mechanism, since otherwise all predictivity is lost.

In conclusion, the robust global χ^2 analysis presented here confirms and quantifies the earlier claims that CSD(3) and CSD(4) represent highly predictive and successful approaches to neutrino mass and mixing models which demand further serious consideration. It is remarkable that such excellent fits for these two cases, with all measured parameters within their one sigma preferred values, can be achieved for simple values of the relative phase $\eta = 2\pi/3$ or $\eta = 4\pi/5$, which could arise due to Z_{3N} or Z_{5N} in realistic models based on CSD(3) or CSD(4), respectively. However in such realistic models we should in general expect further small effects such as charged lepton mixing and renormalisation group corrections to modify somewhat the results presented here.

Finally we have seen that, with just two right-handed neutrinos in CSD(n), there is a direct link between the oscillation phase δ_{CP} and leptogenesis. This is because there is only one phase η appearing in the see-saw mass matrices. Hence η is identified as both the leptogenesis phase in Eq. 5.1 and the phase in the neutrino mass matrix in Eq. 4.1. For a given ordering of right-handed neutrino masses, the sign of η is fixed by the requirement that the observed baryon asymmetry is positive. For instance, if $M_{\text{atm}} \ll M_{\text{sol}}$, then positive baryon asymmetry requires that η is also positive. A

positive η in the neutrino mass matrix implies that δ_{CP} is negative, in agreement with the current hint that $\delta_{CP} \sim -\pi/2$. It is interesting that, for positive η , the global analyses for CSD(3) or CSD(4) with two right-handed neutrinos predict values of $\delta_{CP} \approx -91^\circ$ or $\delta_{CP} \approx -123^\circ$, respectively, with similar predictions when a third approximately decoupled right-handed neutrino is included.

Acknowledgements

We acknowledge support from the European Union FP7 ITN-INVISIBLES (Marie Curie Actions, PITN- GA-2011-289442).

A. CSD(n) from A_4

The basic starting point is to consider some family symmetry such as A_4 which admits triplet representations. The family symmetry is broken by triplet flavons ϕ_i whose vacuum alignment will control the structure of the Yukawa couplings. Consider for example a supersymmetric model, where the relevant superpotential terms that produce the correct Yukawa structure in the neutrino sector are

$$\frac{1}{\Lambda} H_u (L \cdot \phi_{\text{atm}}) \nu_{\text{atm}}^c + \frac{1}{\Lambda} H_u (L \cdot \phi_{\text{sol}}) \nu_{\text{sol}}^c + \frac{1}{\Lambda} H_u (L \cdot \phi_{\text{dec}}) \nu_{\text{dec}}^c \quad (\text{A.1})$$

where L is the SU(2) lepton doublet, assumed to transform as a triplet under the family symmetry, while $\nu_{\text{atm}}^c, \nu_{\text{sol}}^c, \nu_{\text{dec}}^c$ are CP conjugates of the right-handed neutrinos and H_u is the electroweak scale up-type Higgs field, the latter being family symmetry singlets but distinguished by some additional quantum numbers. In the charged-lepton sector,

$$\frac{1}{\Lambda} H_d (L \cdot \phi_e) e^c + \frac{1}{\Lambda} H_d (L \cdot \phi_\mu) \mu^c + \frac{1}{\Lambda} H_d (L \cdot \phi_\tau) \tau^c \quad (\text{A.2})$$

where e^c, μ^c, τ^c are the CP conjugated right-handed electron, muon and tau respectively. The right-handed neutrino Majorana superpotential is typically chosen to give a diagonal mass matrix,

$$M_R = \text{diag}(M_{\text{atm}}, M_{\text{sol}}, M_{\text{dec}}) \quad (\text{A.3})$$

Details of the construction of this superpotential (e.g. in terms of Majoron fields), the relative values of $M_{\text{atm}}, M_{\text{sol}}, M_{\text{dec}}$ as well as the inclusion of any off-diagonal terms in M_R will all depend on the additional specifications of the model.

The CSD(n) vacuum alignments arise from effective operators involving three flavon fields $\phi_{\text{atm}}, \phi_{\text{sol}},$ and ϕ_{dec} which are triplets under the flavour symmetry and acquire VEVs. The subscripts are chosen by noting that ϕ_{atm} correlates with the atmospheric

neutrino mass m_3 , ϕ_{sol} with the solar neutrino mass m_2 , and ϕ_{dec} with the lightest neutrino mass m_1 , which in CSD is light enough that the associated third right-handed neutrino can, to good approximation, be thought of as decoupled from the theory [6]. CSD(n) is defined to be the choice of vacuum alignments,

$$\langle \phi_{\text{atm}} \rangle \propto \begin{pmatrix} 0 \\ 1 \\ 1 \end{pmatrix} \quad \langle \phi_{\text{sol}} \rangle \propto \begin{pmatrix} 1 \\ n \\ n-2 \end{pmatrix} \quad \langle \phi_{\text{dec}} \rangle \propto \begin{pmatrix} 0 \\ 0 \\ 1 \end{pmatrix}, \quad (\text{A.4})$$

where n is a positive integer, and the only phases allowed are in the overall proportionality constants. Such vacuum alignments arise from orthogonality conditions in A_4 as discussed in [16, 17].

Using Eq. A.1, the vacuum alignments in Eq. A.4 make up the columns of the Dirac neutrino Yukawa matrix $Y^\nu \propto (\langle \phi_{\text{atm}} \rangle, \langle \phi_{\text{sol}} \rangle, \langle \phi_{\text{dec}} \rangle)$, giving a Dirac mass matrix

$$m^D = Y^\nu v_u = \begin{pmatrix} 0 & b & 0 \\ a & nb & 0 \\ a & (n-2)b & c \end{pmatrix} \quad (\text{A.5})$$

which is consistent with Eqs. 1.4, 1.5 where $m^D = (m_{\text{atm}}^D, m_{\text{sol}}^D, m_{\text{dec}}^D)$ and the coefficients a , b , and c are generally complex. The charged-lepton Yukawa matrix is chosen to be diagonal (up to model-dependent corrections, assumed small), corresponding to the existence of three flavons ϕ_e , ϕ_μ and ϕ_τ in the charged-lepton sector which acquire VEVs with alignments [16, 17]

$$\langle \phi_e \rangle \propto \begin{pmatrix} 1 \\ 0 \\ 0 \end{pmatrix} \quad \langle \phi_\mu \rangle \propto \begin{pmatrix} 0 \\ 1 \\ 0 \end{pmatrix} \quad \langle \phi_\tau \rangle \propto \begin{pmatrix} 0 \\ 0 \\ 1 \end{pmatrix}. \quad (\text{A.6})$$

Given this choice, it is clear that Y^e is diagonal, hence U_{e_L} is the identity matrix up to diagonal phase rotations, and that $U_{\text{PMNS}} = U_{\nu_L}^\dagger$, i.e. simply the matrix that diagonalises the neutrino mass matrix, up to charged lepton phase rotations.

B. χ^2 near the global minimum

The validity of χ^2 as a test-statistic depends not only on its ability to measure the numerical fit to data but also how reliable its behaviour is in the neighbourhood of a purported global minimum. We find that once we have constrained our parameter space to exclude degenerate minima (corresponding to $\pm\eta$), χ^2 as defined in Section 3 is typically well-behaved near the observed minimum. Fig. 11 shows, for CSD(3) and CSD(4), the variation of χ^2 in this region. Specifically, it plots the lower envelope of χ^2 evaluated for 10^6 vectors in parameter space (m_a, m_b, m_c, η) , chosen randomly.

This means this envelope is not subject to any systematic errors due to any minimising algorithm. Other $\text{CSD}(n)$ alignments do not demonstrate any different behaviours to those observed in these graphs.

The shape of the curves for m_a , m_b , and η show clearly defined minima, while the range of low- χ^2 values is comparatively wider and includes $m_c = 0$. Nevertheless, although m_c may take a large range of values and produce reasonably good χ^2 fits, it appears to have a single minimum region – the global and any local minima are the same. We safely fix the sub-subdominant phase ξ in Fig. 11, which has a negligible effect on the position and nature of the minimum.

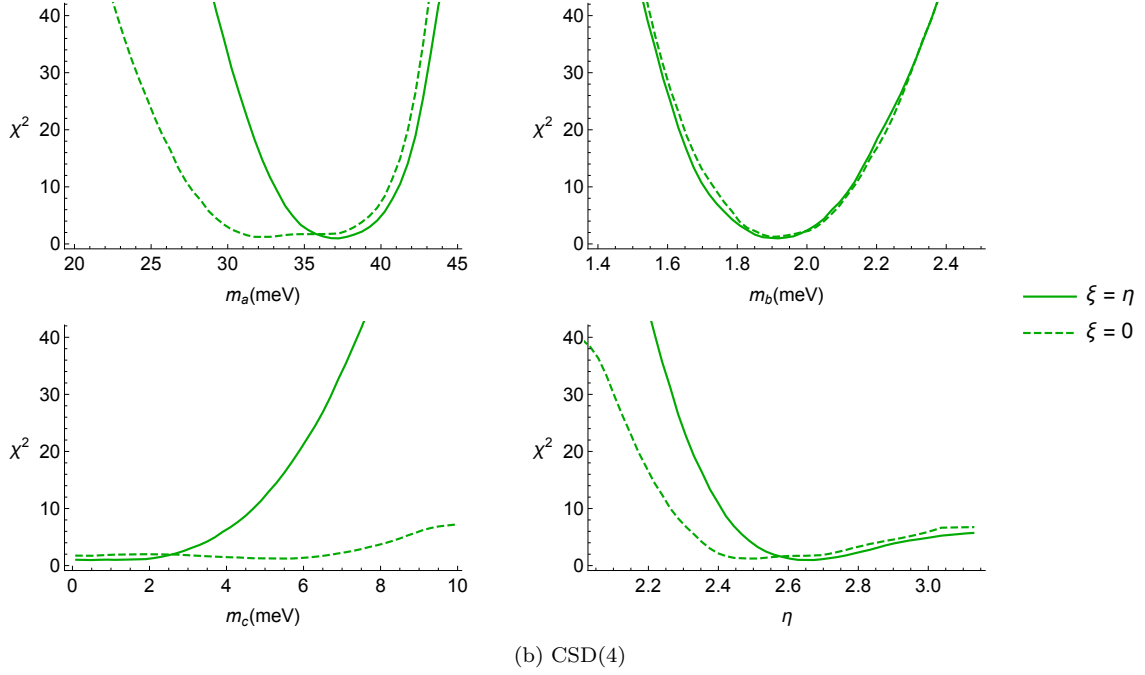
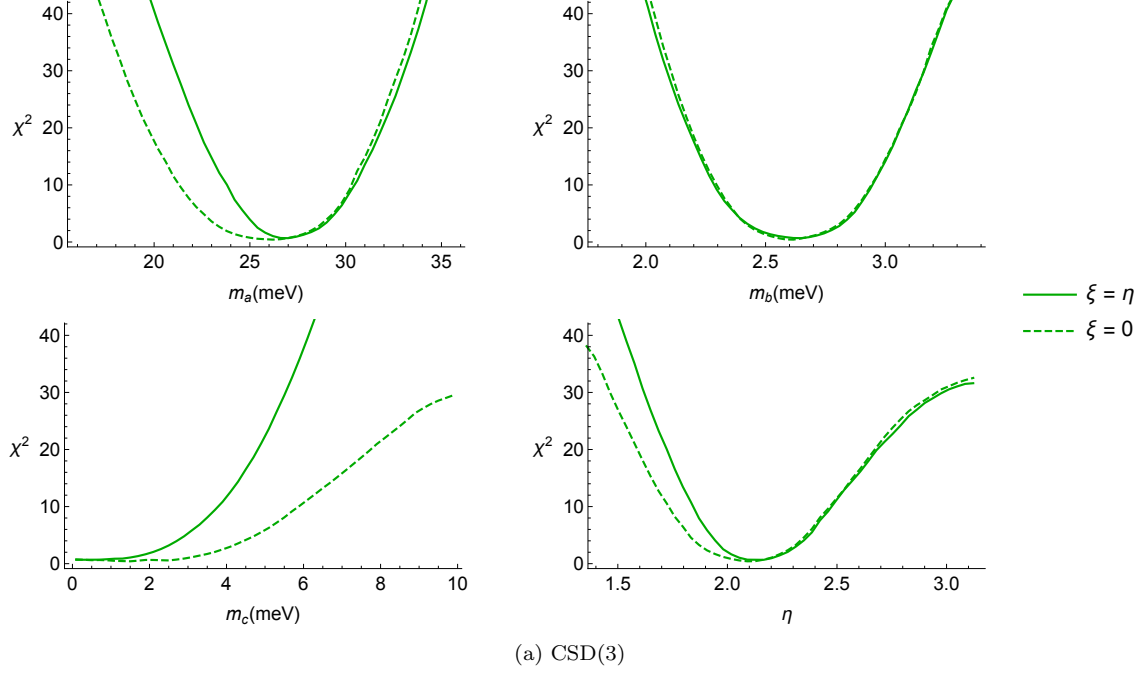


Fig. 11: Lower envelope of best-fit χ^2 in the neighbourhood of the global best-fit of input parameters m_a , m_b , m_c , and η for CSD(3) and CSD(4), with fixed ξ .

References

- [1] F. P. An *et al.* [DAYA-BAY Collaboration], Phys. Rev. Lett. **108** (2012) 171803 [arXiv:1203.1669]; F. P. An *et al.* [Daya Bay Collaboration], Phys. Rev. Lett. **112** (2014) 061801 [arXiv:1310.6732 [hep-ex]]; C. Zhang, “Recent Results From Daya Bay”, talk given at the XXVI International Conference on Neutrino Physics and Astrophysics, Boston, USA, June 27, 2014; J. K. Ahn *et al.* [RENO Collaboration], Phys. Rev. Lett. **108** (2012) 191802 [arXiv:1204.0626]; S.-H. Seo, “New Results from RENO”, talk given at the XXVI International Conference on Neutrino Physics and Astrophysics, Boston, USA, June 27, 2014.
- [2] M. C. Gonzalez-Garcia, M. Maltoni and T. Schwetz, JHEP **1411** (2014) 052 [arXiv:1409.5439 [hep-ph]].
- [3] D. V. Forero, M. Tortola and J. W. F. Valle, arXiv:1405.7540.
- [4] F. Capozzi, G. L. Fogli, E. Lisi, A. Marrone, D. Montanino and A. Palazzo, Phys. Rev. D **89** (2014) 093018 [arXiv:1312.2878].
- [5] P. Minkowski, Phys. Lett. B **67** (1977) 421; T. Yanagida, in Proceedings of the Workshop on Unified Theory and Baryon Number of the Universe, eds. O. Sawada and A. Sugamoto (KEK, 1979) p.95; P. Ramond, Invited talk given at Conference: C79-02-25 (Feb 1979) p.265-280, CALT-68-709, hep-ph/9809459; M. Gell-Mann, P. Ramond and R. Slansky, in Supergravity, eds. P. van Nieuwenhuizen and D. Freedman (North Holland, Amsterdam, 1979) Conf.Proc. C790927 p.315, PRINT-80-0576.
- [6] S. F. King, Phys. Lett. B **439** (1998) 350 [hep-ph/9806440]; S. F. King, Nucl. Phys. B **562** (1999) 57 [hep-ph/9904210]; S. F. King, Nucl. Phys. B **576** (2000) 85 [hep-ph/9912492];
- [7] S. F. King, JHEP **0209** (2002) 011 [hep-ph/0204360]; S. F. King, Phys. Rev. D **67** (2003) 113010 [hep-ph/0211228].
- [8] G. Altarelli and F. Feruglio, Rev. Mod. Phys. **82**, 2701 (2010) [arXiv:1002.0211 [hep-ph]].
- [9] H. Ishimori, T. Kobayashi, H. Ohki, Y. Shimizu, H. Okada and M. Tanimoto, Prog. Theor. Phys. Suppl. **183**, 1 (2010) [arXiv:1003.3552 [hep-th]]; Lect. Notes Phys. **858**, 1 (2012); Fortsch. Phys. **61**, 441 (2013).
- [10] S. F. King and C. Luhn, Rept. Prog. Phys. **76** (2013) 056201 [arXiv:1301.1340].
- [11] S. F. King, A. Merle, S. Morisi, Y. Shimizu and M. Tanimoto, New J. Phys. **16** (2014) 045018 [arXiv:1402.4271].

- [12] S. F. King and G. G. Ross, Phys. Lett. B **520** (2001) 243 [hep-ph/0108112];
S. F. King and G. G. Ross, Phys. Lett. B **574** (2003) 239 [hep-ph/0307190].
- [13] S. F. King, JHEP **0508** (2005) 105 [hep-ph/0506297].
- [14] M. C. Chen and S. F. King, JHEP **0906** (2009) 072 [arXiv:0903.0125 [hep-ph]];
S. F. King, JHEP **1101** (2011) 115 [arXiv:1011.6167 [hep-ph]].
- [15] S. Antusch, S. F. King, C. Luhn and M. Spinrath, Nucl. Phys. B **856** (2012) 328
[arXiv:1108.4278 [hep-ph]];
- [16] S. F. King, JHEP **1307** (2013) 137 [arXiv:1304.6264 [hep-ph]].
- [17] S. F. King, Phys. Lett. B **724** (2013) 92 [arXiv:1305.4846 [hep-ph]].
- [18] S. F. King, JHEP **1401** (2014) 119 [arXiv:1311.3295 [hep-ph]]; S. F. King, JHEP
1408 (2014) 130 [arXiv:1406.7005 [hep-ph]].
- [19] S. F. King and C. Luhn, JHEP **0910** (2009) 093 [arXiv:0908.1897].
- [20] M. Holthausen, K. S. Lim and M. Lindner, Phys. Lett. B **721** (2013) 61
[arXiv:1212.2411 [hep-ph]].
- [21] S. F. King, T. Neder and A. J. Stuart, Phys. Lett. B **726** (2013) 312
[arXiv:1305.3200 [hep-ph]]; S. F. King and T. Neder, Phys. Lett. B **736** (2014)
308 [arXiv:1403.1758 [hep-ph]].
- [22] L. Lavoura and P. O. Ludl, Phys. Lett. B **731** (2014) 331 [arXiv:1401.5036 [hep-ph]].
- [23] R. M. Fonseca and W. Grimus, JHEP **1409** (2014) 033 [arXiv:1405.3678 [hep-ph]].
- [24] T. Araki, H. Ishida, H. Ishimori, T. Kobayashi and A. Ogasahara, Phys. Rev. D **88**
(2013) 096002 [arXiv:1309.4217 [hep-ph]]; H. Ishimori and S. F. King, Phys. Lett.
B **735** (2014) 33 [arXiv:1403.4395 [hep-ph]]; H. Ishimori, S. F. King, H. Okada and
M. Tanimoto, arXiv:1411.5845 [hep-ph].
- [25] S. Antusch, J. Kersten, M. Lindner, M. Ratz and M. A. Schmidt, JHEP **0503**
(2005) 024 [hep-ph/0501272].
- [26] K.A. Olive et al. (Particle Data Group), Chin. Phys. C **38**, 090001 (2014).
- [27] F. Feruglio, K. M. Patel and D. Vicino, JHEP **1409** (2014) 095 [arXiv:1407.2913
[hep-ph]].
- [28] S. Antusch and M. Spinrath, Phys. Rev. D **79** (2009) 095004 [arXiv:0902.4644 [hep-
ph]].

- [29] P. A. R. Ade *et al.* [Planck Collaboration], *Astron. Astrophys.* **571** (2014) A16 [arXiv:1303.5076 [astro-ph.CO]].
- [30] P. Di Bari, *Contemp. Phys.* **53** (2012) 4, 315 [arXiv:1206.3168 [hep-ph]]; S. Blanchet and P. Di Bari, *New J. Phys.* **14** (2012) 125012 [arXiv:1211.0512 [hep-ph]].
- [31] S. Antusch, S. F. King and A. Riotto, *JCAP* **0611** (2006) 011 [hep-ph/0609038].
- [32] S. F. King, *Nucl. Phys. B* **786** (2007) 52 [hep-ph/0610239].
- [33] E. E. Jenkins and A. V. Manohar, *Phys. Lett. B* **668** (2008) 210 [arXiv:0807.4176 [hep-ph]]; E. Bertuzzo, P. Di Bari, F. Feruglio and E. Nardi, *JHEP* **0911** (2009) 036 [arXiv:0908.0161 [hep-ph]]; D. Aristizabal Sierra, F. Bazzocchi, I. de Medeiros Varzielas, L. Merlo and S. Morisi, *Nucl. Phys. B* **827**, 34 (2010) [arXiv:0908.0907].
- [34] S. Choubey, S. F. King and M. Mitra, *Phys. Rev. D* **82** (2010) 033002 [arXiv:1004.3756].
- [35] S. F. King, *Phys. Rev. D* **67** (2003) 113010 [hep-ph/0211228].
- [36] S. Antusch, P. Di Bari, D. A. Jones and S. F. King, *Phys. Rev. D* **86** (2012) 023516 [arXiv:1107.6002 [hep-ph]].
- [37] P. Di Bari, L. Marzola and M. R. Fiorentin, arXiv:1411.5478 [hep-ph]; P. Di Bari and L. Marzola, *Nucl. Phys. B* **877** (2013) 719 [arXiv:1308.1107 [hep-ph]]; P. Di Bari and A. Riotto, *JCAP* **1104** (2011) 037 [arXiv:1012.2343 [hep-ph]].
- [38] P. Di Bari and S. F. King, in preparation.